JOURNAL OF MATERIALS SCIENCE 21 (1986) 1591–1600

Acetone intercalation/de-intercalation processes in the HUP ($H_3OUO_2PO_4 \cdot 3H_2O$) framework: a model for electrochemical degradation

M. PHAM-THI*
Laboratoire de Physico-Chimie et Dispositifs Ioniques, LCR Thomson–CSF, Domaine de Corbeville 91401, Orsay, France

Ph. COLOMBAN‡
Groupe de Chimie du Solide, LPMC, Ecole Polytechnique, 91128 Palaiseau, France

Intercalation of acetone molecules in the $H_3OUO_2PO_4 \cdot 3H_2O$ framework has been studied by X-ray diffraction, differential scanning calorimetry and IR and Raman spectroscopies. The influence of water traces in acetone is pointed out. Four main phases are observed in the course of the rehydration/de-intercalation process. The nature of proton bonding with the $(UO_2PO_4)_n$ slab and its evolution are discussed (H_3O^+, PO_4^{3-}, HPO_4^{2-}, HPO_4^{2-} . . .). The presence of defects in the sub-stoichiometric HUP is demonstrated. Comparison is made with similar partially dehydrated material obtained under electric field action in electrochemical solid state devices.

1. Introduction

HUP ($H_3OUO_2PO_4 \cdot 3H_2O$) materials exhibit some interesting properties: superionic protonic conductivity [1], ferroelectricity [2], ionic exchange [3] and the ability to intercalate large organic species, i.e. cobaltocene [4]. Thus this material is used in microionic devices such as electrochromic displays [5, 6] hydrogen sensors [7, 8] and supercapacitors [9, 10].

In previous studies the influence of preparative conditions on structural defects and conducting properties as well as the intercalation of acetone molecules have been demonstrated [4, 11]. However, the acetone treatment is often used by scientists to dry powders and its influence on the materials is neglected [12, 13]. Thus in the course of a comprehensive study of water non-stoichiometry and the influence of structural defects on conducting properties we have studied the acetone intercalation/de-intercalation and dehydration/hydration processess. The possibility of observing the different steps of the process led us to establish the modification of the structure precisely. Furthermore, degradation of the material in electrochemical devices could be brought to light by these studies.

In this paper we present vibration (IR and Raman spectroscopies), differential scanning calorimetry and X-ray diffraction studies of the acetone intercalation/de-intercalation process. The influence of water traces in acetone is underlines.

2. Experimental details

HUP was prepared from 2.3 M phosphoric acid and uranyl nitrate solution as described elsewhere [14]. Deuterated samples were prepared by isotopic exchange in a D_2O atmosphere at room temperature and subsequent drying as previously described. Acetone treatments were performed in closed vessels, and rehydration in atmospheric air (relative humidity $\sim 60\%$). Different kinds of acetone were used:

Acetone HPLC (Prolabo): water content $< 0.1\%$
Acetone RP (Prolabo): water content $\sim 0.25\%$
Acetone RP: water content $\sim 1\%$
Acetone RP: water content $\sim 5\%$

The HUP/acetone volume ratio was 5 to 10/1000. Deuterated acetone was also used.

The composition of the initial HUP material, given by the formula $H_3O(UO_2)_{0.98\pm0.02}PO_4 \cdot (3 \pm 0.05)H_2O$, was determined by chemical analysis and careful measurement of water content using differential scanning calorimetry (DSC) and combined thermogravimetric analysis. Infrared spectra of suspensions of crystalline powders in Nujol and Fluorolube using CsI, CaF_2 and TPX windows were recorded at various temperatures between 100 and 300 K on a 783 Perkin–Elmer spectrophotometer. Raman spectra were studied on an RTI 30 Dilor (Lille, France) triple monochromator apparatus in the 100 to 300 K temperature range; the 647.1 nm line of a Spectra Physics (Palo

Present address: Laboratoire d'Analyse Physique, LCR Thomson–CSF, Domaine de Corbeville 91401, Orsay, France.
‡To whom correspondence should be addressed.

0022–2461/86 $03.00 + .12

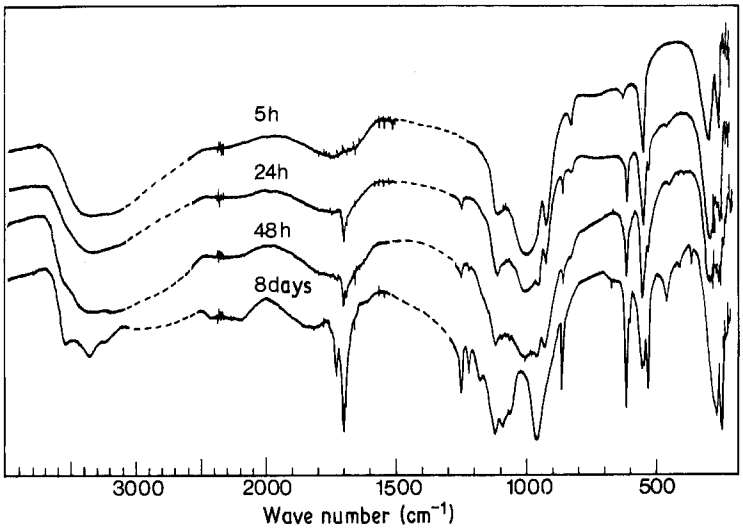

Figure 1 Infrared evidence for gradual transformation of $H_3OUO_2PO_4 \cdot 3H_2O$ material into α' phase $(UO_2HPO_4)(CH_3COH_3)H_2O$.

Alto, California) krypton laser of about 300 mW was selected as the exciting line.

Differential scanning calorimetry was performed using a DSC4 Perkin–Elmer instrument between 200 and 600 K.

Conductivity measurements were made using the complex impedance method using a Solartron (Schlumberger Inc.) apparatus monitored by an Apple II microcomputer.

3. De-intercalation of acetone molecules and structural modifications

3.1. Existence of various phases

Fig. 1 shows the evolution of the IR spectra of HUP powder as a function of the dipping duration in acetone containing traces of water (~ 1 wt %). Strong modifications occur in all regions of the vibrational spectra, indicating a structural change involving both UO_2^{2+}, PO_4^{3-} and $H_2O(H_3O^+)$ species.

Fig. 2 gives X-ray powder patterns for the two cases observed (with or without H_2O traces). Well-crystallized materials are obtained.

The HUP original structure consists of infinite sheets of UO_2PO_4 entities (each UO_2 ion is coordinated with four PO_4 ions) separated by a two-level water molecule layer; oxygen atoms of this layer are on squares and each water molecule may be included in four hydrogen bonds (Fig. 3). The inter-slab distance is equal to 0.875 nm. The assumption that the material remains a lamellar compound during the acetone intercalation/de-intercalation process is based on the four following remarks:

(i) the bonds withint the $(UO_2PO_4)_n$ slab are stronger than the hydrogen bond between a water layer and a $(UO_2PO_4)_n$ slab [14];

(ii) the crystallite habit remains in the form of platelets [11];

(iii) large molecules or cations can be intercalated without drastic change of the $(UO_2PO_4)_n$ slab;

(iv) ionic homologues (NaUP, KUP . . .) can be reversibly dehydrated without change of the $(UO_2PO_3)_n$ slab [4].

This assumption is consistent with the X-ray patterns given in Fig. 2. As previously observed in the case of alkyl ammonium ionic exchange, the presence of water in acetone has a drastic influence [4], but in the case of acetone containing 5% H_2O no more modification of the HUP framework is observed. On the other hand two kinds of situation are observed in the case of "water-free" acetone ($< 0.1\%$ wt %) or in the case of acetone containing about 1 wt % H_2O, respectively.

Interpretation of the X-ray powder patterns with a lamellar feature gives an inter-slab distance of 0.97 nm (phase α) and 1.08 nm (phase α'), respectively. These inter-slab distances are consistent with the presence of acetone (without or with extra water) molecules, the inter-slab distances being of the same order of magnitude as those observed for small alkylammonium ions [4, 15].

Different phases are observed in the course of the gradual restoration of the usual HUP structure. Four phases are recognized, called α, β, γ and δ, respectively (α', β', γ and δ in the case of acetone containing H_2O traces).

In order to specify this evolution precisely, DSC runs were performed after different exposure durations to atmospheric moisture. Simultaneously the volatile species contents below 60° C and below 300° C were measured. Results are given in Figs. 4 and 5. As indicated on X-ray patterns, four different phases are recognized. The absolute height of each 0 0 l peak gives an estimate of the material crystallinity, and the plot is given in Fig. 5. Phases $\alpha(\alpha')$ and δ are relatively well crystallized, whereas the γ phase is highly disordered. The emphasis will be laid on phase δ. Its X-ray powder pattern just differs a little from the HUP one (mainly a broadening of the 1 1 2 peak at 0.432/0.4365 nm and of the 0 0 2 peak, on the high spacing side.). In the literature different phases of HUP have been mentioned [16–18]: Type I with a P4/n c c space group is the frequently often observed polymorph; Type III with space group P4/n m m has only been observed by Ross [17] and Williams [18], whereas a monoclinic distorsion (Type II) has only been obseved by Moroz *et al.* [16]. In a previous study [11] we have pointed out the possible syntaxy of different structures having different compositions (i.e. $UO_2(H_2PO_4)_2 \cdot 3H_2O$, $(UO_2)_3(PO_4)_2 \cdot 4H_2O$ . . .) during the precipitation, which makes hypothetical the

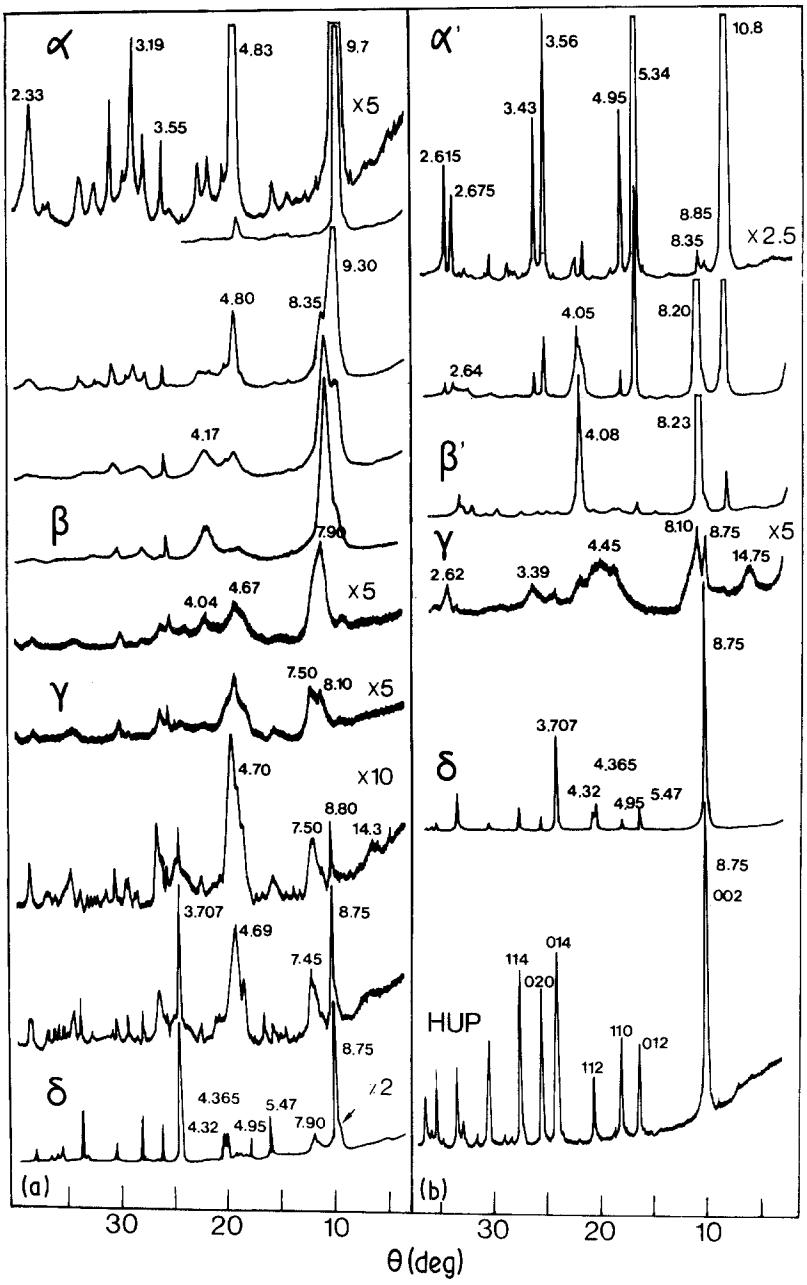

Figure 2 Evolution of X-ray powder patterns (Cu$K\alpha$ radiation) during the de-intercalation process: (a) for water-free acetone, (b) for acetone containing traces of H_2O. Spacings are given in Å (1 Å = 0.1 nm).

existence of various phases having the same composition. However, a water stoichiometry variation without modification of the U/P ratio, induced by acetone treatment (or electrochemical cycling) modifies the X-ray spectra and "different" HUP species could be recognized, in the absence of accurate study. However, the packing of uranium atoms gives the major part of the X-ray intensity, and X-ray powder spectra are not very sensible to the modification of protonic species.

3.2. Proton transfer and acetone intercalation in the $\alpha(\alpha')$ phase

We first discuss the α- ("water-free") acetone phase. As shown in Fig. 5, this phase is only stable in the presence of a high acetone partial pressure. Gravimetric measurements indicate a composition of between 1 and 2 acetone molecules per HUP. When the last molecules leave the structure, the inter-slab distance decreases from 0.97 to 0.96 nm to 0.93 nm, and the β phase appears (d = 8.3 nm). On DSC traces, the peak at about 50 to 60° C is asigned to the departure of the acetone molecules.

Fig. 6 compares the OH and CH stretching and bending regions for the different phases. Fig. 7 gives the corresponding Raman spectra of the α-acetone intercalated phase and of deuterated homologues ($D_3O^+UO_2PO_4 \cdot 3D_2O$ in CD_3COCD_3). Traces of hydrogen-bond free acetone molecules, absorbed on the crystallites, are visible (νC–O at 1722 cm^{-1}, for example) that disappear in one minute. On the other hand the strong band at about 1705 cm^{-1}, which shifts gradually to 1680 cm^{-1}, is assigned to intercalated, strongly hydrogen-bonded acetone molecules [19].

Simultaneously an ABC pattern is observed (2850, 2300, 1700 cm^{-1}; see Tables I and II for frequencies and assignements) characteristic of an HPO_4^{2-} species [20, 21].

Figs. 8 and 9 compare IR and Raman spectra in the UO_2PO_4 mode region. The spectra of deuterated homologues have previously been given in a preliminary report [4]. A strong distorsion of UO_2 packing

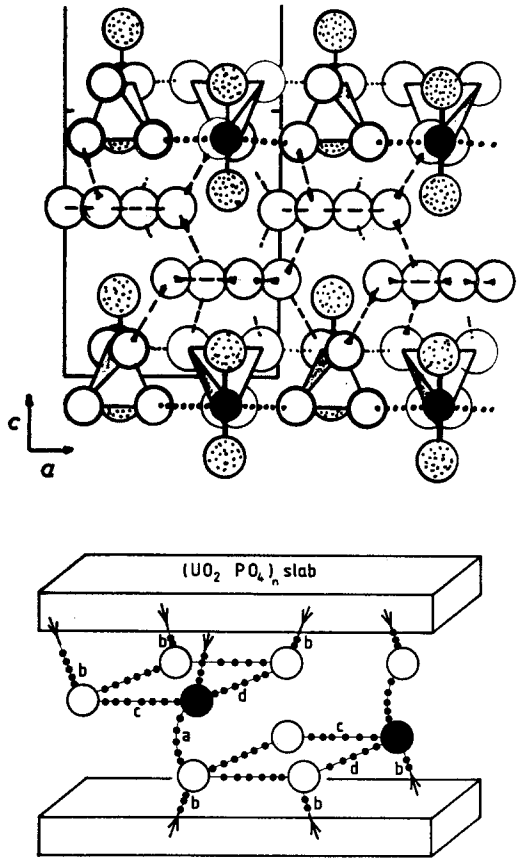

Figure 3 Projection along the (0 1 0) direction of the HUP structure and diagrammatic representation of a water layer. (○) $H_2O(O_4)$, (●) $H_3O^+(O_4')$, (†) $PO_4(O_3)$, (. . .) hydrogen bond.

is observed: the $\nu_1 UO_2$ mode is intense in the IR spectrum, which corresponds to an asymmetric UO_2^{2+} ion. The high $\nu_1 UO_2$ frequency (865 cm^{-1}) indicates a softening of the UO_2–PO_4 equatorial bonding. This is consistent with the formation of well-separated

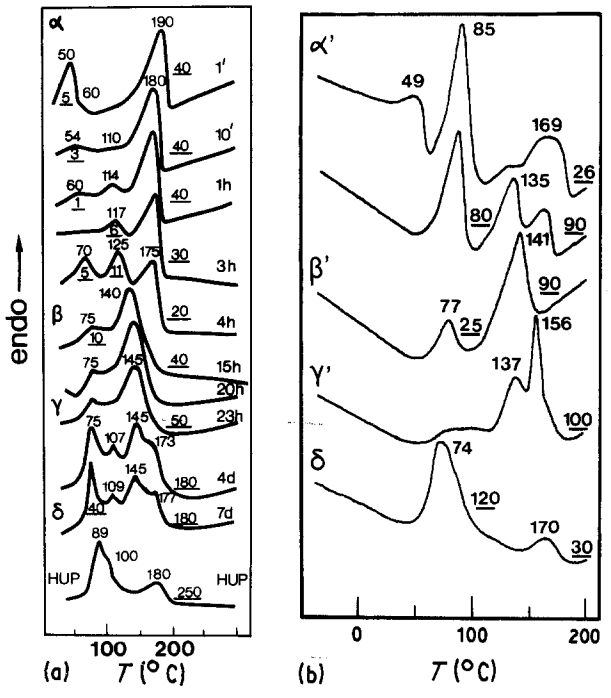

Figure 4 Evolution of the DSC traces as a function of the duration of exposure to atmospheric moisture: (a) water-free acetone, (b) acetone with traces of H_2O. Heating rate 20° C min^{-1}. ΔH is given in cal g^{-1} (1 cal = 4.187 J).

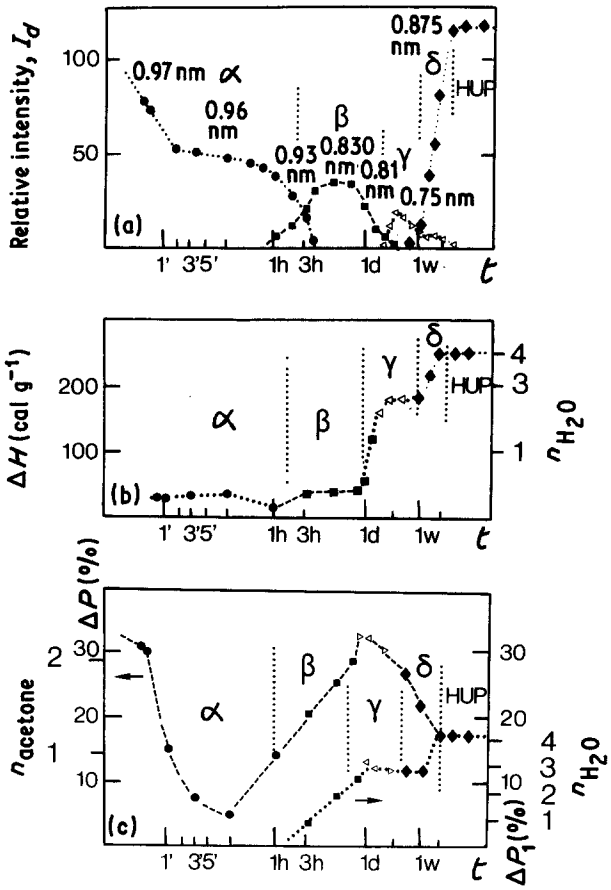

Figure 5 Kinetics of the rehydration and acetone de-intercalation process as a function of the duration of moisture exposure: (a) X-ray intensity (height) plot of the inter-slab distances, (b) values of the total ΔH measured on DSC traces, (c) total weight loss (ΔP) for a 300° C heating cycle and weight loss occurring between 60 and 300° C (ΔP_1). 1 cal = 4.187 J.

νPO_2(~950 cm^{-1}) and $\nu P(OH)_2$ modes (1085, 1115 cm^{-1}). They shift appropriateely on deuteration and on $P^{18}O_4/P^{16}O_4$ substitution (Table III).

The presence of water traces modifies the pattern of the ABC band and the frequencies are shifted to higher values (3000, 2400, 1820 cm^{-1}) and extra bands (3350, 3540 cm^{-1}) are assigned to the water species. The presence of water molecules between the UO_2PO_4 slabs increases the inter-slab distance (1.08 nm) and the hydrogen bonding between HPO_4 and acetone molecules is reduced. No other strong modification is noticed in the 200 to 1200 cm^{-1} region. The conductivity decreases ($\sigma \sim 10^{-5}\Omega^{-1}cm^{-1}$ at 300 K).

The presence of HPO_4 species is consistent in DSC runs of the α phase with the existence of a 190° C peak, as observed in the parent compounds $UO_2(H_2PO_4)_2 \cdot 3H_2O$, $(UO_2)_{1.5-x}H_{2x}PO_4 2H_2O$ [11, 21, 22]. In the α' phase, the 85° C peak could be assigned to the extra water molecules. Thus the following formula could be proposed:

α phase: $(UO_2HPO_4)\ (CH_3COCH_3)_x$ $\quad x \sim 1$

α' phase: $(UO_2HPO_4)\ (CH_3COCH_3, H_2O)_x$ $\quad x \sim 1$

3.3. The intermediate β(β') phase

Fig. 6 shows that acetone molecules are no longer present in the material (disappearance of the δCH_3 modes in the 1300 to 1450 cm^{-1} region). Simultaneously the intensity of the ABC feature is strongly reduced

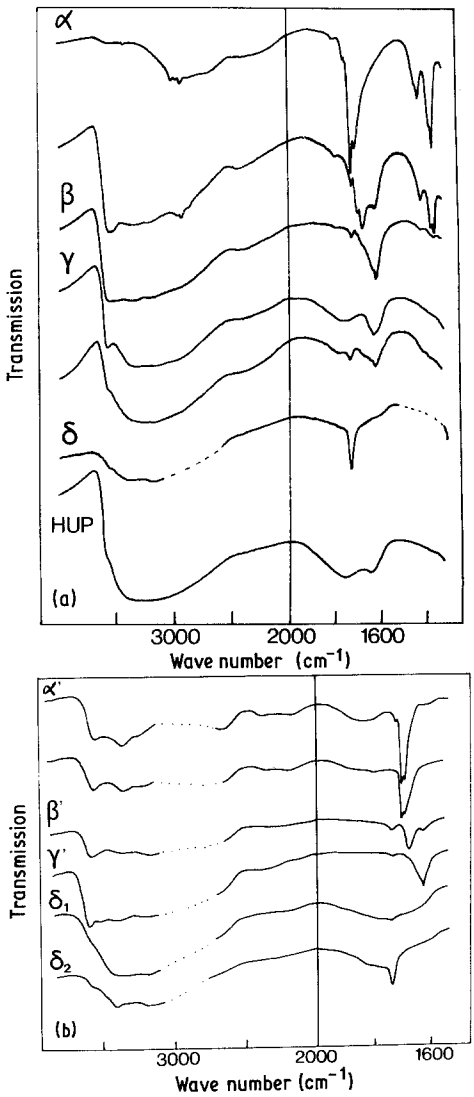

Figure 6 Typical IR spectra recorded in the 1500 to 4000 cm^{-1} region as a function of exposure to a moist atmosphere: (a) for water-free acetone, (b) for acetone with traces of H_2O.

and an intense νOH broad band is observed above 3000 cm^{-1}.

A broad pattern at 1740 cm^{-1} (as in HUP) is observed, especially in the β' phase. As far as the $(UO_2PO_4)_n$ framework modes are concerned, the intenstity of the $\nu_1 UO_2$ mode is lowered and all the other modes are broadened.

On DSC traces, peaks at about 75 and 140° C are observed by comparison with results for other structures; this is consistent with the presence of H_3O^+ and HPO_4 species. The proposed formula is

$$(UO_2H_xPO_4)(H_3O)_{1-x}H_2O \quad 0 < x < 1$$

The structure is lamellar. The presence of water traces shifts the reaction to higher x values.

3.4. The highly disordered γ phase

This phase is highly disordered, as shown by X-ray powder patterns. The material is highly hydrophilic (Fig. 5c): a lot of water molecules ($> 5H_2O$ molecules per UO_2PO_4 are absorbed on crystallites (well-defined bands at 3580 and 1635 cm^{-1}) and perhaps between $(UO_2PO_4)_n$ slabs (Bragg peaks at 1.45 to 1.48 nm are observed). Simultaneously a strong modification of the UO_2PO_4 framework occurs: the $\nu_1 UO_2$ mode is shifted from 860 to 850 cm^{-1}, which indicates an increasing metal–ligand U...(PO_4) bonding. The 480 cm^{-1} IR mode, previously assigned to this mode [14] is well defined. The νPO_3 and νP(OH) modes are largely separated. The IR spectrum is intermediate between those observed for $(UO_2)_3(PO_4)_2 \cdot 4H_2O$ and for $(UO_2)_{1.5-x}H_xPO_4 \cdot 2H_2O$ [11]. It is possible that this important re-ordering of the $(UO_2PO_4)_n$ slabs corresponds to changes in the UO_2 equatorial coordination. In fact in some situations (i.e. $UO_2(H_2PO_4)_2 \cdot 3H_2O$), a pentagonal coordination is observed (four PO_4 tetrahedra and one water molecule), and the material is green-fluorescent as in the case of α and β phases. On the other hand in HUP and in the γ and S phases, powders are yellow. A possible formula is $(UO_2H_xPO_4)H_3O_{1-x} \cdot 4H_2O$ with $x \ll 1$.

3.5. δ phase or sub-stoichiometric HUP

This phase appears relatively similar to normal HUP, as far as only the X-ray powder pattern is concerned. This is consistent with a very similar UO_2/PO_4 arrangement. UO_2 and PO_4 vibrational modes are also nearly unchanged. However, IR bands at about 1270 and 1080 to 1120 cm^{-1} (HUP_0^*) or 1400 and 1115 to 1170 cm^{-1} (HUP) as well as a 470 to 480 cm^{-1} mode appear slightly more intense than in normal HUP [14]. A stronger difference is observed in the ν and δOH region (Fig. 6): the most important feature is the narrow well-defined band at 1735 cm^{-1}. In some cases this band is not visible at 300 K and becomes visible below 0° C. Simultaneously the 480 cm^{-1} band and that at 1074 to 1120 cm^{-1} are narrowed and become more intense. After a cooling cycle, the spectra remain unchanged at room temperature for a few hours.

The 1735 cm^{-1} narrow band could be assigned to H_3O^+ ions in an isolated configuration. The 1750 cm^{-1} broad band is shifted to 1800 cm^{-1}, indicating a more hydrogen-bonded $H_2O(H_3O^+)$ species, as observed in the low-temperature IR spectra of normal HUP.

On the other hand, modes observed in the 1050 to 1300 cm^{-1} region shift to lower frequency on $P^{18}O_4/P^{16}O_4$ substitution and could be assigned to POH modes.

The following assumption is made: water vacancies are present in the water layer slab and H_3O^+ ions could be located at the centre of a water square, the surrounding molecules being either absent or totally hydrogen-bonded with other species (PO_4, H_3O^+, H_2O) in another water square. Thus the H_3O^+ ion under consideration is hydrogen-free and its bandwidth is narrower. Thermal cycling or exposure to atmospheric moisture induces a disappearance of the defects.

Fig. 10 compares DSC traces for different phases in the + 10 to − 50° C range, where water-layer ordering occurs in HUP [14, 23]. In the δ phase the broadness of the DSC peak is appreciable, which agrees with a higher degree of disorder. In the γ phase, the peak is broader still. By comparison, in HUP the DSC traces are narrow.

3.6. Electrochemical degradation of HUP

As mentioned at the begining of the paper, HUP is used

TABLE I νOH and νCH bands in the 1000 to 4000 cm^{-1} range (low water traces) at room temperture*

Assignment	α phase				β phase	γ phase	δ phase		HUP	Assignment
	DUP		HUP		HUP	HUP	δ_1 IR	δ_2 IR	IR	
	IR	Raman	IR	Raman	IR	IR				
νH_2O						3580 m	3590 sh	3590 sh		
			3250 vw		3480 s					
			3430 vw		3420 sh					
					3380 s	3380 s, b	3400 s	3360 s, b	3350 s, b	
					3200 s	3200 s, b	3180 s, b	3180 s, b		νOH (H_2O, H_3O^+)
νHPO_4	2700 m, b		2850 m, b	2950 m, b	2900 sh	2900 sh				
(νDPO_4)							2600 sh	2600 sh	2600 sh	
	2300 m, b		2300 m, b		2300 w	2300 sh	2300 sh	2300 sh	2300 sh	
νCH_3	2260 w	2260 w	3015 w	3010 w						
(νCD_3)	2140 w	2225 vw	2970 vw	2975 vw						
		2200 vw								
	2155 w	2115 m	2935 w	2930 m						
$\nu C{=}O$			1800 vw		1790 vw					
			1750 vw							
		1730 w	1722 s		1720 vw					
			1705 m	1705 vw						
	1670 s, b	1675 s	1680 sh	1685 s	1680 m					
δH_2O			1620 sh	1550 w, b	1620 s	1635 s, b	1630 sh	1630 sh	1640 sh	δH_2O
						1760 m, b	1800 m, b	1760 m, b		
							1735 s	1735 sh	1740 s, b	δH_3O^+
δCH_3				1450 m						
			1440 sh	1440 w, b						
			1425 m		1420 vw					
			1375 sh							
			1366 m		1365 vw	traces				
				1355 w						
						1405 w	1405 w			
$\nu C{-}C$	1275 s		1246 m	1240 vw						
	1225 s		1222 m		1220 vw					
									1160 sh	δH_3O^+

*s: strong, m: medium, w: weak, sh: shoulder, v: very, b: broad.

in microionic devices. Fig. 11 compares the electrolyte spectra after two different cycling conditions under an electric field imposed using a polarizable blocking electrode (a description of the apparatus is given elsewhere [10]); in the first example (2 V a.c. potential, frequency 1 Hz, two weeks) as well as in the second one (100 V a.c., 1 Hz, two weeks) modification of the electrolyte is clearly evident.

TABLE II νOH and νCH bands in the 1000 to 4000 cm^{-1} range (high water traces) at room temperature*

Assignment	α' phase HUP	β' phase HUP
νH_2O	3540 m	3570 m
	3350 m	3350 m
		3190 m
νHPO_4	2800 m	2900 sh
	2390 w, b	2300 vw, b
	2180 w, b	
	1860 m, b	
$\nu C{=}O$		1740 w
	1725 w	
	1702 s	
	1690 sh	1680 m
δH_2O	1610 sh	1620 w
$\nu C{-}C$		1260 vw
	1246 m	
	1216 w	

*s: strong, m: medium, w: weak, v: very, sh: shoulder, b: broad.

As in the δ phase, a mode at 1735 cm^{-1} is seen in the first case. Simultaneously a well-defined mode at 1100 cm^{-1} is evident. Cooling at 100 K induces a broadening, and after a few hours at room temperature in atmospheric moisture as well as in water–Nujol mulls, the usual spectrum of HUP is restored. The most probable explanation is that the δ phase has been formed under the action of the electric filed and the subsequent electrochemical reactions

$$H_2O \rightleftharpoons 2H^+ + \tfrac{1}{2}\uparrow O_2 + 2e$$

$$H_2O + 2e \rightleftharpoons O_2^- + \uparrow H_2$$

occurring as a function of polarity, each 1 second. Thus formation of H_2O vacancies occurs and the substoichiometric δ phase is formed.

High voltages induce a more pronounced evolution of the $(UO_2PO_4)_n$ framework. IR spectra of the cycled electrolyte are similar to those of $UO_2(H_2PO_4)_2 \cdot 3H_2O$; H_2PO_4 species must be formed. This could be related to composition modifications and defect formation induced by reactions such as

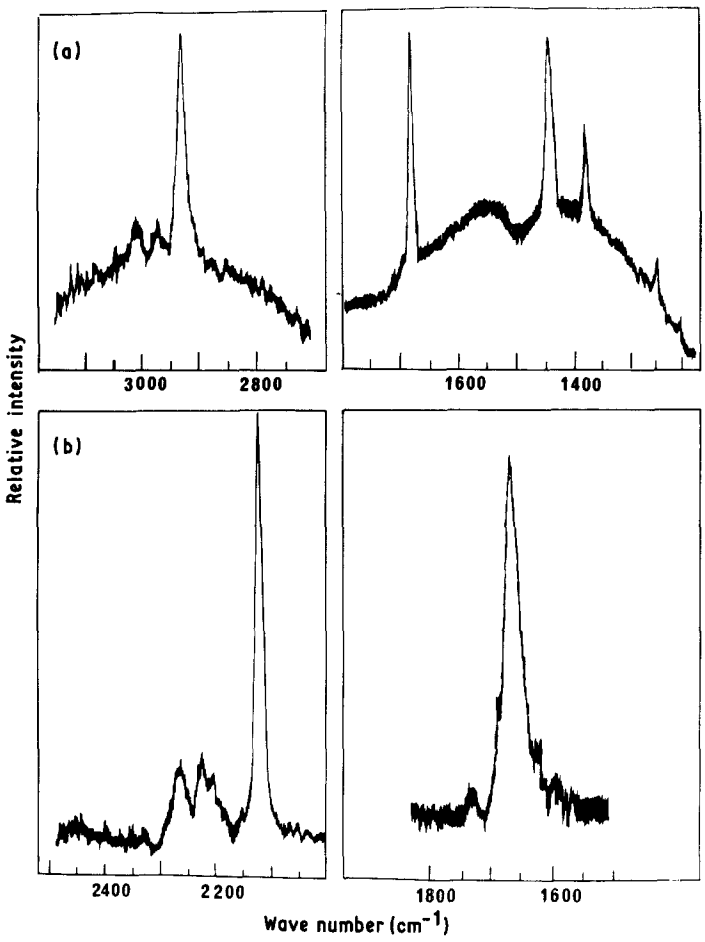

Figure 7 νCH and νC=O Raman spectra for acetone molecules intercalated in the (a) αHUP and (b) DUP phases.

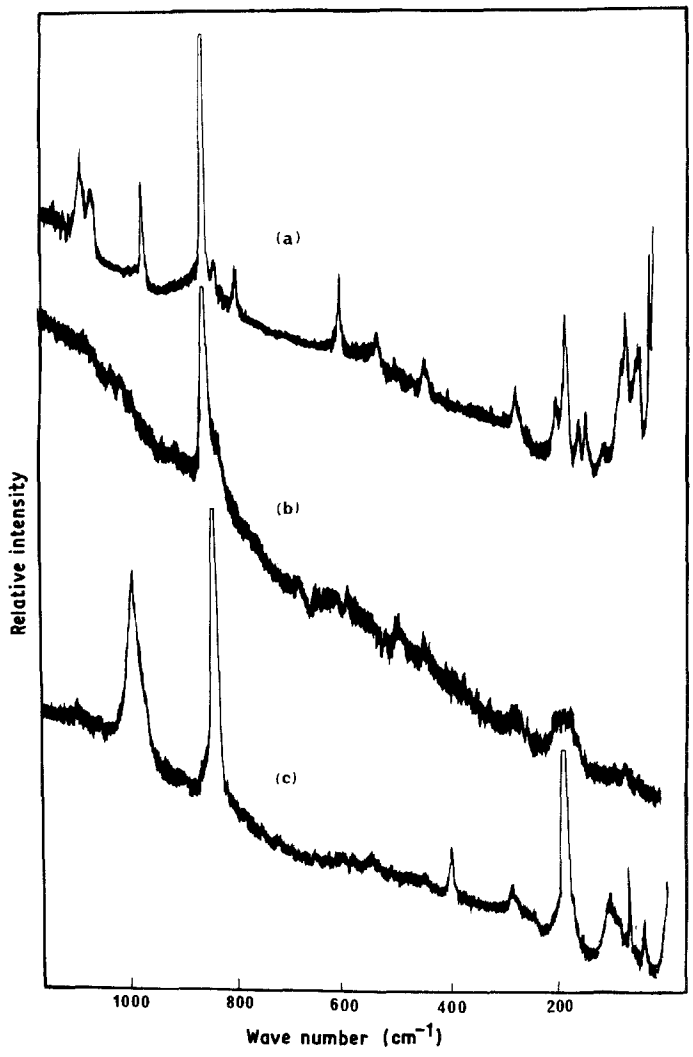

Figure 8 Comparison of Raman spectra of (a) α phase, (b) γ phase and (c) normal HUP phase.

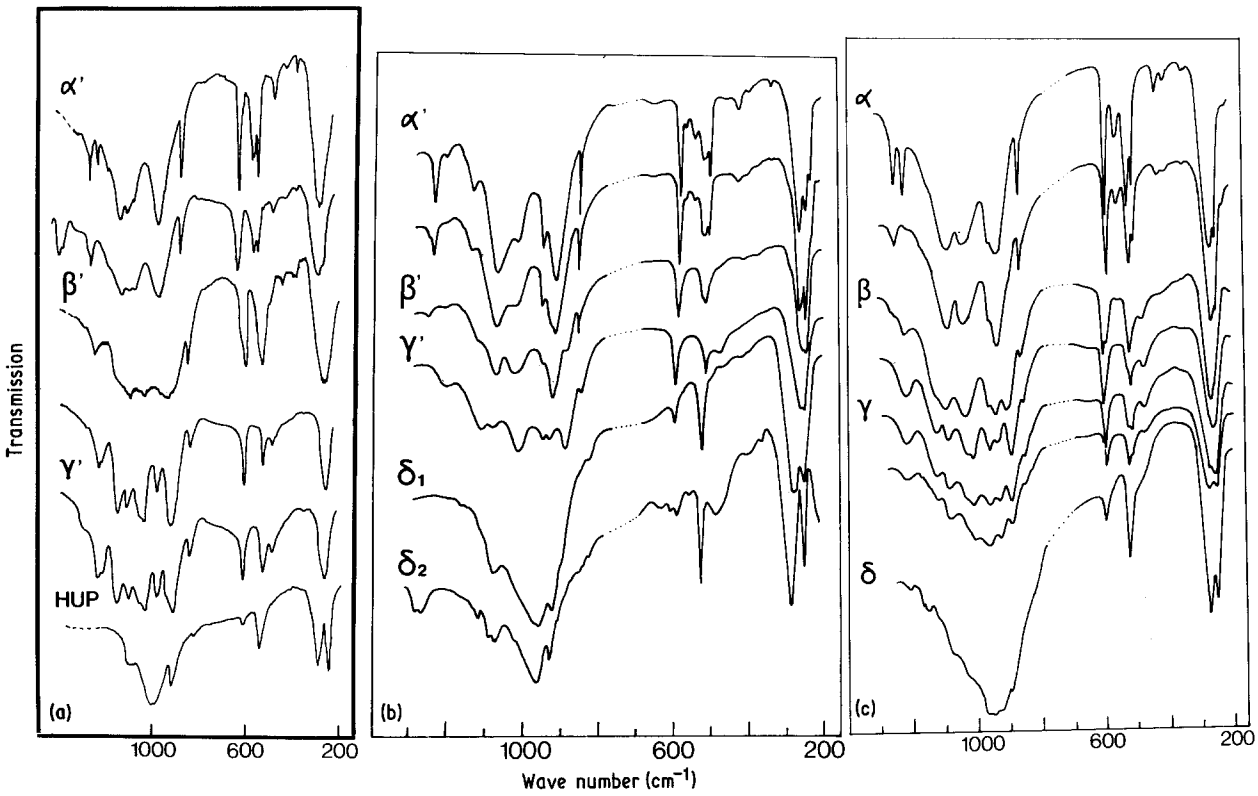

Figure 9 IR spectra of different steps recorded during the rehydration process in the framework mode region: (a) acetone-intercalated HUP, (b) HUP* ($H_3OUO_2P^{18}O_4 \cdot H_2O$) in the presence of water traces, (c) water-free acetone-intercalated HUP*.

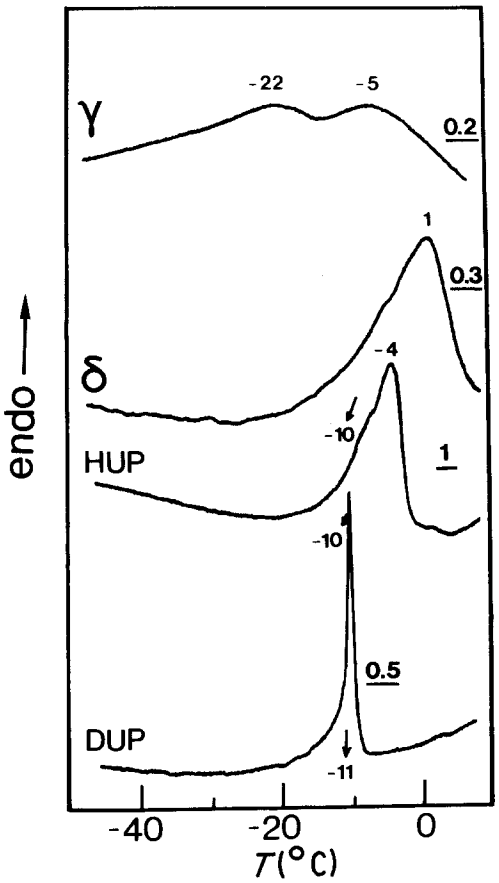

Figure 10 Comparison of DSC traces for the different phases γ, δ and HUP (DUP) in the temperature range where water-layer ordering occurs. Heating rate 20°C min^{-1} after a 200°C min^{-1} cooling cycle.

$$UO_2^{2+} + e \rightleftharpoons UO_2^{+}$$

or

$$2H_3O^{+} + PO_4 \rightharpoonup H_2PO_4 + 2H_2O$$

More precise description of the electrochemical degradation is in progress.

4. Conclusion

HUP is a lamellar hydrate composed of relatively rigid $(UO_2PO_4)_n$ slabs, separated by protonated water molecule layers. Thus modification of the "active" layer can take place without drastic modification of the $(UO_2PO_4)_n$ slab. Immersion in acetone induces intercalation of acetone molecules, proton transfer from H_2O^+ species to the PO_4 framework and subsequent dehydration. Rehydration/acetone de-intercalation is a step which involved reorganization of the water layer as well as of the $(UO_2PO_4)_n$ slab. The formation of defects in the water layer (isolated H_2O^+ ions and/or POH species) is pointed out in the case of sub-stoichiometric HUP (δ phase). The conductivity is thus modified. The metastability of this phase and its hydrophilic behaviour are pointed out.

Various modifications of the crystallite habit are observed during the rehydration process as a function of water partial pressure [11]. Acetone drying appears to be a "soft" method to study materials similar to those formed in electrochemical solid state devices. Furthermore, reorganization of the framework in the course of the dehydration/rehydration process gives a model for master reactions occuring in the case of the synthesis of oxides from the inorganic polymerization of alkoxides [24].

TABLE III Framework modes in the 10 to 1200 cm^{-1} domain (low water ratio) at room temperature†

Assignment	α phase						β phase		γ phase		δ_2 phase			δ_1 phase	
	DUP		HUP		HUP*		HUP	HUP*	HUP	HUP*	HUP	HUP*		HUP	HUP*
	IR	Raman	IR	Raman	IR	Raman	IR	IR	IR	IR	IR	IR	Raman	IR	IR
νHPO_4															1290 m
							1255 m	1220 m	1246 m	1210 m	1250 w	1210 vw		1170 w	1270 m
	1200sh		1175sh		1170sh						1170w	1170sh		1160w	
				1145w	1150sh				1150s		1115m	1150w		1120sh	
	1130sh	1110s	1115s				1150sh		1118s	1118m		1125sh		1108m	1122w
			1090s	1098s	1075m		1112s	1080s		1080m		1080sh		1095s	1095m
	1065s	1070m	1060s	1077s	1035m										1075m
		1030w							1050s	1010s		1025sh		1010sh	
		1005vw					1050s	1025s	985s	955s	997s	960s	960m	980s	965s
	965vs	967m	950vs	978s	955sh		950s	955sh	950sh	930m	922m	920sh		925w	930w
νUO_2	900sh	900w	930sh		926vs		920sh	930s	925s	885s	850sh	890sh	865w		
					890sh			895s	846s	848w	825sh	850sh	843vs	855sh	850sh
	863m	875vs	860m	865vs	860m	865vs	859w	862w				825sh		825w	830sh
		715m		845w	770vw	810vw									
							620sh		620s	600m	620w	600w		655vw	635w, b
														625w	612w
														615m	598w
δHPO_4			625sh				608s	602s							
	610s	603m	610s	608m	590m	580m		590sh							
			550s	550m	558w										
	545s		545sh						646s	526m	545m	525m		550m	529m
	530s	528w	530s	535m	520m	510w	540s	520s		518sh					
	510m(ac)				508m				495m	478w, b	480sh	480sh, b		510w, b	488m, b
														470sh	
$\nu U–O–PO_3$							490sh	480m, b							400sh
δHPO_4	450w	435m	450w	445m	423w	415w	440vw								
	410vw	410w	400vw	400w	408w										
	360vw	360w	360vw	377m	350vw		390vw								
	340vw	340w													
	280vs	270m	275vs		255s	250m	265s	265s	270sh	265s	285s	278s		300s	285s
$\nu_2 UO_2$	250sh	255w	250sh		250sh		250sh	250sh	250s		250m	250m		255m	252m
$R'UO_2$		210w, b		200m											
		180s		182s		180s							205s		
Lattice modes	a	160sh	a	155m	a		a	a	a	a	a	a		a	a
		135m		143m		115w									
		105m		110vw									90m, b		
		77m		75sh									78m		
		60m		65s		70w							50m		
				43s											
				20w											

†s: strong, m: medium, w: weak, sh: shoulder, v: very, b: broad, ac: acetone, HUP* = $H_3OUO_2P^{18}O_4 \cdot 3H_2O$, a = frequency range not studied.

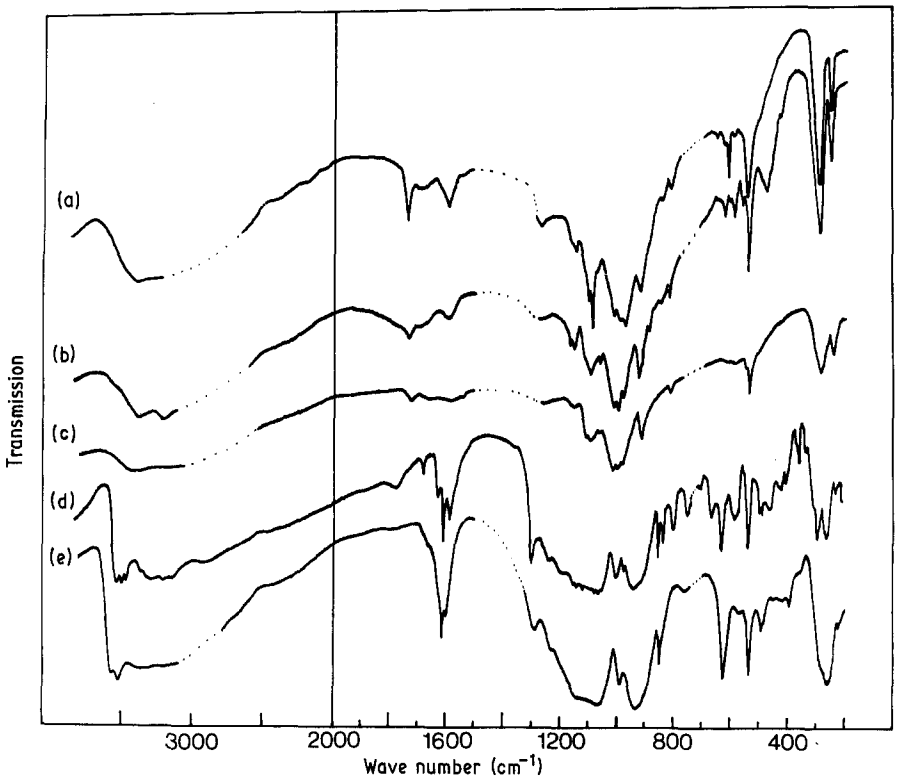

Figure 11 IR spectra at various temperatures of HUP discs under (a, b, c) 2 V or (d, e) 100 V cycling: (a) immediately after cycling; (b) spectrum at nitrogen temperature; (c) spectrum at room temperature, 2 h later; (d) immediately after cycling (spectrum recorder at room temperature); (e) spectrum recorded at nitrogen temperature.

Acknowledgements

Dr A. Novak is thanked for his comments and for the use of his laboratory's facilities. Mrs N. Blanchard is kindly thanked for her technical assistance during this work.

References

1. M. G. SHILTON and A. T. HOWE, *Mater. Res. Bull.* **12** (1977) 701.
2. M. A. R. de BENYACAR and H. L. de DUSSEL, *Ferroelectrics* **9** (1975) 241.
3. M. ROSS and H. T. EVANS, *Amer. Mineral.* **49** (1964) 1578.
4. Ph. COLOMBAN and M. PHAM-THI, *Rev. Chim. Minérale* **22** (1985) 143.
5. A. T. HOWE, S. H. SHEFFIELD, P. E. CHILDS and M. G. SHILTON, *Thin Solid Films* **67** (1980) 365
6. M. PHAM-THI and G. VELASCO, *Solid State Ionics* **14** (1984) 217
7. G. VELASCO, H. PERTHUIS and Ph. COLOMBAN, in Proceedings of the International Meeting on Chemical Sensors, Fukuoka, Japan, September 1983, edited by T. Seiyama, K. Fueki, J. Shiokawa and S. Suziki, (Elsevier, 1983) p. 239.
8. J. S. LUNDGAARD, J. MALLING and M. L. S. BIRCHALL, *Solid State Ionics* 7 (1982) 53.
9. G. VELASCO, M. PHAM-THI and Ph. COLOMBAN, French Patent No. 8509653 (1985).
10. M. PHAM-THI, Ph. ADET, G. VELASCO and Ph. COLOMBAN, *Appl. Phys. Lett.* in press.
11. M. PHAM-THI and Ph. COLOMBAN, *J. Less-Common Metals* **108** (1985) 189.
12. K. D. KREUER, W. WEPPNER and A. RABENAU, *Solid State Ionics* **3/4** (1981) 353.
13. H. KAHIL, M. FORESTIER and J. GUITTON, in "Solid State Protonic Conductors III", edited by J. B. Goodenough, A. Potier and J. Jensen (Odense University Press, 1985) p. 356.
14. M. PHAM-THI, Ph. COLOMBAN and A. NOVAK, *J. Phys. Chem. Solids.* **46** (1985) 565.
15. A. V. WEISS, K. HARTL and U. HOFMANN, *Z. Nat. Forsch.* **12b** (1957) 669.
16. I. Kh. MOROZ, A. A. VALUEVA, E. A. SIDORENKO, L. G. SHILTOSAVA and L. N. KORPOVA, *Geokhimya* (1973) 210.
17. V. ROSS, *Amer. Mineral.* **40** (1955) 917.
18. G. R. WILLIAMS, *Bull. Inst. Geochem. Astrom. Univ. Sao Paulo* **2** (1971) 83.
19. P. V. HUONG and G. NOEL, *Spectrochim. Acta* **32A** (1978) B31.
20. D. HADZI, S. BRATOS, in "The Hydrogen Bonds", edited by P. Schuster, G. Zundel and C. Sandorfy, (North-Holland, Amsterdam, 1976) p. 565.
21. R. MERCIER, M. PHAM THI and Ph. COLOMBAN, *Solid State Ionics* **15** (1985) 113.
22. P. PIRET and M. DELIENS, *Bull. Mineral.* **105** (1982) 125.
23. Ph. COLOMBAN, M. PHAM-THI and A. NOVAK, *Solid State Commun.* **53** (1985) 747.
24. J. P. BOILOT and Ph. COLOMBAN, *J. Mater. Sci. Lett.* **4** (1985) 22.

Received 28 May
and accepted 20 June 1985